DEUTSCHES ELEKTRONEN-SYNCHROTRON DESY

DESY 83-098
Oktober 1983

MONTE CARLO SIMULATIONS WITH SYMANZIK'S IMPROVED ACTIONS IN THE LATTICE O(3) NON-LINEAR σ-MODEL

by

B. Berg and I. Montvay

II. Institut für Theoretische Physik, Universität Hamburg

S. Meyer

Fachbereich Physik der Universität Kaiserslautern

ISSN 0418-9833

NOTKESTRASSE 85 2 HAMBURG 52

To be sure that your preprints are promptly included in the
HIGH ENERGY PHYSICS INDEX ,
send them to the following address (if possible by air mail) :

DESY
Bibliothek
Notkestrasse 85
2 Hamburg 52
Germany

DESY 83-098
Oktober 1983

ISSN 0418-9833

Monte Carlo Simulations with Symanzik's Improved Actions in the Lattice O(3) Non-linear σ-Model

by

B. Berg [1], S. Meyer [2] and I. Montvay [1,3]

Abstract The scaling properties of the lattice O(3) non-linear σ-model are studied. The mass-gap, energy-momentum dispersion, correlation functions are measured by numerical Monte Carlo methods. Symanzik's tree-level and 1-loop improved actions are compared to the standard (nearest neighbour) action.

1) II. Institut für Theoretische Physik der Universität Hamburg

2) Fachbereich Physik der Universität Kaiserslautern;
supported by Deutsche Forschungsgemeinschaft

3) Supported by Bundesministerium für Forschung und Technologie

Introduction

In the last years considerable work was spent in Monte Carlo (MC) simulations of euclidean field theories. Sources of systematic errors and limitations to numerical simulations are:

a) statistical noise;

b) finite size effects;

c) finite lattice spacing effects.

Exact block spin renormalization group transformations allow to simulate an L^d lattice on an $(\frac{L}{n})^d$ lattice, where n^d (typically n = 2) is the block size and L a multiple of n. The lattice spacing on the new lattice is (n a) in units of the lattice spacing a of the L^d lattice, and this transformation can, of course, be iterated. The price paid is the introduction of many new interactions, which in general cannot be calculated analitically. Monte Carlo renormalization group (MCRG) techniques /1,2/ use a truncated ansatz for the new interactions and try a numerical determination. In principle the above limitations (b) and (c) can be improved, but in practice statistical noise (a) is a severe problem. To the 2d O(3) non-linear σ-model Wilson's /2/ MCRG version has been applied by Shenker and Tobochnik /3/.

More recently Symanzik /4,5/ suggested a systematic procedure for constructing lattice actions, which minimize the cutoff dependence (c), and approach more rapidly the continuum limit. There are many possible actions on the lattice which formally converge to the same continuum limit when the lattice spacing $a \to 0$. In the case of renormalizable interactions, for small lattice spacing, a given action on the lattice is equivalent to a local theory on the continuum with a local effective Lagrangian

$$\mathcal{L}_{eff} = \mathcal{L}_0 + a^2\mathcal{L}_1 + a^4\mathcal{L}_2 + \cdots \qquad (I.1)$$

$\mathcal{L}_0$ is the ordinary renormalizable continuum Lagrangian in d dimensions, $\mathcal{L}_1$ contains operators of dimension d+2, etc.. Because of "irrelevant" operators the renormalization group equations contain non-universal scaling violating terms. n-point Green-functions calculated on the lattice obey

$$\left\{-a\frac{\partial}{\partial a}+\bar{\beta}(g)\frac{\partial}{\partial g}+n\bar{\gamma}(g)\right\}G_n(p_1,\dots,p_n;g,a)= \\ = O(a^2\ln a) \quad . \tag{I.2}$$

The suggestion of Symanzik is to choose the lattice action in such a way that the r.h.s. of equation (2) is at most of order $O(a^4\ln a)$. In the 2d O(N) non-linear sigma model the improved action has the following form /4/:

$$\begin{aligned} S_{imp} = -g^{-1}a^2\sum_j \Big\{ & \left(-\tfrac{1}{2}\phi K\phi + \mathcal{F}\phi\right) + \\ & + a^2\mathcal{F}\left[c_1\phi(\phi K\phi)+c_2 K\phi\right] + a^2c_3(\mathcal{F}\phi)^2 + \\ & + a^2c_4\mathcal{F}^2 + a^2c_5(K\phi)^2 + a^2c_6\sum_\mu\left[\partial_\mu\partial_\mu^+\phi\right]^2 + \\ & + a^2c_7(\phi K\phi)^2 + a^2c_8\sum_\mu\left[\phi\partial_\mu\partial_\mu^+\phi\right]^2 + \\ & + a^2c_9\sum_{\mu,\nu}\left[\frac{\partial_\mu+\partial_\mu^+}{2}\phi\cdot\frac{\partial_\nu+\partial_\nu^+}{2}\phi\right]^2\Big\} . \end{aligned} \tag{I.3}$$

Here the O(N)-vectors $\phi\equiv\phi_j$ on lattice sites j are normalized to unity: $\phi^2 = 1$, and the following notation is used:

$$\partial_\mu\phi_j = a^{-1}(\phi_{j+\hat{\mu}}-\phi_j) \; ; \qquad \partial_\mu^+\phi_j = a^{-1}(\phi_j-\phi_{j-\hat{\mu}}) \; ;$$

$$K = -\sum_{\mu=1}^{2}\partial_\mu\partial_\mu^+ \quad . \tag{I.4}$$

We often use $\beta = {}^1/g$.

The Green-functions are obtained by differentiating $Z_{imp} = \int[d\phi]\exp(-S_{imp})$ with respect to the source vector J. The improved field, for instance, is

$$\phi^{imp}_{j\alpha} = \phi_{j\alpha} + c_1\phi_{j\alpha}(\phi K\phi) + c_2 K\phi_{j\alpha} \quad , \tag{I.5}$$

where α is the O(N) index.

The improvement coefficients $c_i(g,N)$ can be determined in perturbation theory, in ${}^1/N$ expansion or, in principle, also by Monte Carlo checks of scaling ("trial and error"). For the standard action (SA) all coefficients c_i (i = 1, ..., 9) are zero. The perturbatively tree-level improved action (TIA) has been calculated by Martinelli et al. /6/. Defining

$$c_i = c_i^0 + c_i^1 g + c_i^2 g^2 + \dots \quad , \tag{I.6}$$

the tree level result is

$$c_6^0 = -\frac{1}{24} \tag{I.7}$$

and all other $c_i^0 = 0$. The TIA does not improve the 4-point functions to one loop order.

For comparison we note that Shenker and Tobochnik /3/ did a spin wave fit to the block spin renormalization group. They were lead to the interaction term which we encounter for the TIA, however, with $c_6^{\,o} = -\,{}^1/10$.

Symanzik /5/ has calculated the one loop improved action (1LIA). One encounters in it two free parameters. We make here the same choice ($c_3^{\,1} = c_7^{\,1} = 0$) as in Ref. /7/, where also the relevant numerical integrals are explicitly given. For the convenience of the reader our final coefficients $c_i^{\,1}$ are listed in Table 1. They differ slightly from those of Ref. /5/, but stay within the class of actions for which the improvement $O(a^2 \ln a) \to O(a^4 \ln a)$ of equation (I.2) can be theoretically achieved. It is instructive to rewrite our 1LIA in the lattice notation

$$S = \sum_{i=1}^{3} b_i S_i^b + \sum_{i=1}^{10} q_i S_i^q \quad . \tag{I.8}$$

The first sum goes over all bilinear and the second sum over all quadrilinear interaction terms. Coefficients, and interaction terms are listed in Tables 2. The one loop corrections to b_1 is notably large in the β -region available for MC simulations.

MC simulations with the 1LIA action were carried out in Ref. /7/, and for the TIA action by Falcioni et al. /8/. In the present paper we present more details and considerable extensions of the previous investigation /7/. We describe the used MC methods and summarize our statistics in section II. Most of our results are obtained on a 50^2 lattice. In section III, we present our continuum mass gap estimates and in section IV, we study the energy-momentum dispersion for states of momentum $K = \frac{2\pi n}{L}$, n = 0, 1, ..., 10. Section V, contains our results for the magnetic succeptibility and a 4-point function. The latter is inconclusive because of statistical noise. We have also taken MC data for the two-point function at non-zero momenta.

In the 2d O(N) non-linear sigmal model the $\bar{\beta}$ - and $\bar{\gamma}$ -functions of equation (I.2) have universal (regularization scheme independent) parts /9/:

$$\bar{\beta}_{univ}(g) = -\frac{(N-2)}{2\pi} g^2 - \frac{(N-2)}{4\pi^2} g^3 \quad , \tag{I.9}$$

$$\bar{\gamma}_{univ}(g) = \frac{(N-1)}{2\pi} g \; . \tag{I.10}$$

The universal parts are obtained from a 2-loop calculation in any regularization. Continuum estimates of the mass gap (cf. section III) use the Λ -scale as obtained from the universal $\bar{\beta}$ -function, and try to establish a scaling window (cf. Ref. /10/ for a more detailed discussion). We will call this <u>asymptotic scaling</u> (valid for g, $a \to o$ asymptotically). More generally <u>scaling</u> means: Equation (I.2) holds with some function $\bar{\beta}(g)$ and the r.h.s. = 0. Scaling but not neccesarily asymptotic scaling is improved by using Symanzik actions. Even if scaling holds, higher perturbative (3-loop, ...) corrections to the $\bar{\beta}$ - and $\bar{\gamma}$ -functions could spoil asymptotic scaling in an intermediate coupling constant range. In mass ratios (or other dimensionless quantities) these perturbative corrections drop out, and we expect improvement. For instance in the equation

$$\frac{m_1}{m_2} = \text{const} \cdot \{ 1 + O(a^2 \ln a) \}$$

the correction on the r.h.s. is improved to $O(a^4 \ln a)$.

In section VI, we analyse our results with respect to scaling in the sense of equation (I.2). This is enabled by the fact that we have measured a considerable number of higher momentum states. In the final section VII, we summarize our results and draw some conclusions.

II. The Monte Carlo Statistics

In this section we summarize our MC data. A review of the MC method is given in Ref. /11/. For bilinear (spin) interactions the heat bath method is very efficient. Upgrading of a spin $\vec{s} = \vec{s}_j$ amounts to replacing it by a new spin $\vec{s}'$ which is selected with the probabilistic Boltzmann weight

$$e^{\beta \vec{s}' \vec{S}} \quad ; \qquad \vec{S} = \sum a_j \vec{\phi}_j \tag{II.1}$$

where the sum involves all spins interacting with $\vec{s}$. More precisely $\vec{s}\,\vec{S}$ is the contribution of spins involving $\vec{s}$ to the total action.

In our investigation we have used the heat bath method for the SA and the TIA. For the SA $\vec{S}$ is a sum of four terms and for the TIA $\vec{S}$ is a sum of eight terms. As most of the computer time is spent in calculating $\vec{S}$ with the weight (II.1), upgrading the TIA is only slightly ($\sim$ 1.2) slower than upgrading the SA.

In case of the 1LIA the quadrilinear interaction terms (cf. Table 2.b) prevent us from applying the heat bath method. We have used Metropolis with 4 hits per trial. The upgrading procedure is roughly 5 times slower than for the SA. We perform measurements of all considered observables after each sweep. A sweep consists in upgrading each spin of the lattice once in the mean; we did random upgrading (cf. Ref. /10/, section II.a). For all three actions measurements take about the same time. In case of the 1LIA measurements took roughly $^1/3$ of the used computer time, one sweep and measurements is only by a factor 2.5 slower than for the SA. The Metropolis upgrading is, however, clearly less efficient than heat bath upgrading, therefore the error bars are larger.

Together with mean values for the average link action

$$E \overset{\text{def}}{=} \langle 1 - \phi_j \phi_{j+\hat{\mu}} \rangle , \tag{II.2}$$

our final statistics is collected in the Tables 3. At the beginning we did always 2000 sweeps without measurements, for reaching equilibrium. At identical β-values the results for E are clearly distinct for the three different actions, in particular TIA and 1LIA are notably different. We always calculate our error-bars by dividing our complete statistics into 10 bins. Typically this amounts to groups of 2000 events. For the SA at β = 1.4, 1.5 we have also results on a 100^2 lattice. All other calculations were done on a 50^2 lattice. At β = 0.8 we have also used the Metropolis upgrading for the TIA and checked it against results with the heat bath upgrading. Within statistical errors we found perfect agreement.

III. The Mass Gap

In this section we present our results for the mass gap. We also compare with previously reported mass gap estimates /3, 12-17/.

We obtain upper bounds on the mass gap from correlations between momentum zero eigenstates

$$c(\Delta t) = \langle \vec{\tilde{\phi}}(t)\, \vec{\tilde{\phi}}(t+\Delta t) \rangle , \qquad \text{(III.1)}$$

where

$$\vec{\tilde{\phi}}(t) = \sum_{x=0}^{L-1} \vec{\phi}(x,t) . \qquad \text{(III.2)}$$

In case of the 1LIA the improved field (I.5) is taken. For our analysis we use the mass gap definition

$$m(\Delta t) = -\frac{1}{\Delta t} \ln \left| \frac{c(\Delta t)}{c(0)} \right| , \quad (\Delta t = 1, 2, \ldots) . \qquad \text{(III.3)}$$

In case of nearest-neighbour interactions, we have a transfer matrix T, which connects nearest neighbour time planes. If the transfer matrix is bounded from below (not necessarily positive definite), we obtain upper bounds on the mass gap from the MC values for $m(\Delta t)$. If the transfer matrix is positive definite $m(\Delta t)$, $\Delta t \to \infty$ will decrease monotonically against the real mass gap. Otherwise oscillations due to complex eigenvalues of the transfer matrix are possible. In the latter case it is dangerous to use the mass gap definitions (cf. for instance Ref. /10/)

$$\hat{m}(\Delta t_1, \Delta t_2) = -\frac{1}{\Delta t_2 - \Delta t_1} \ln \frac{c(\Delta t_2)}{c(\Delta t_1)} ,$$

$$(\Delta t_1, \Delta t_2 = 1, 2, \ldots ; \Delta t_2 > \Delta t_1) .$$

For the TIA and 1LIA one has to generalize the concept of the transfer matrix, because of next-nearest neighbour interactions. Now also next neighbour time planes become connected and we can trust $m(\Delta t)$ to be an upper bound only for $\Delta t \geq 2$. This is not an academic question, as for the TIA the $m(1)$ value is in general the lowest.

Our MC results rely on the statistics outlined in section II. We have measured all possible correlations, this means $t = 0, 1, \ldots, \frac{L}{2}$, $(L = 50, 100)$. To illustrate our method for extracting the mass gap, we give in Table III.1 all calculated correlations for some selected values of β. Table III.2 contains the $m(\Delta t)$ mean values, which are obtained from these correlations. In case of the 1LIA we have taken the correlations of the improved field (I.5). For the final results error bars are calculated (by the method of section II) from the error bars of the relevant $C(\Delta t)$, neglecting the error bar of $C(0)$ becuase of correlations. For large Δt the error bars of $C(\Delta t)$ increase and finally reliable results can no longer be obtained.

The values $m(\Delta t)$ $(\Delta t = 1(2), \ldots, \frac{L}{2})$ are upper bounds for the mass gap. As long as $m(\Delta t)$ is rather stable under going to larger values Δt, we believe to obtain a good approximation to the mass gap (at the β-value in question). If the

correlation length ξ becomes too large, we enter (on a finite lattice) the spin wave region, and no sensible value for the mass gap can be extracted. In this case a power law behaviour is indicated for the correlation function $C(\Delta t)$, $\Delta t \to \infty$ by strongly decreasing values for $m(\Delta t)$ as $\Delta t \to \infty$. For the SA on the 50^2 lattice we illustrate this at $\beta = 1.6$, where the correlation length is $\xi \cong 20$.

Our final mass gap results are summarized in Fig. II.1. The Λ-parameters of this figure are defined by ($\beta = \beta_S, \beta_{TI}, \beta_{1LI}$)

$$\Lambda_L^{S,I} = 2\pi\beta \exp(-2\pi\beta)\left(1 + O(1/\beta)\right) \quad , \tag{III.4}$$

S = standard, I = improved. The O(g) coefficients, distinguishing TIA and 1LIA, do not affect the asymptotic Λ-scale Λ_L^I. The full lines of Fig. I.1 are approximate continuum estimates. For the TIA the full line is taken from Ref. /8/. and our MC data are seen in good agreement with it. For the SA we have taken a value which is consistent with previous MC literature /3, 12-14/. In this case the discrepancies in the literature are, however, large and the status of asymptotic scaling is now obscured by Ref. /14/.

In Fig. II.2 we plot the defects

$$d = \text{const}\ \frac{m}{\Lambda_L^{S,I}} \tag{III.5}$$

versus $\ln \xi$, where ξ is the correlation length. (The constants in (III.5) are adjusted such that always $d(\beta = 0.8) = 1.0$.) We clearly find improvement in the sense that the mass gap exhibits asymptotic scaling already at a very small correlation length for the 1LIA. For the SA we have on a lattice of the same size (50^2) no signal at all for asymptotic scaling. To some extent this result is a surprise, because Symanzik's improvement is concerned with scaling and not

(at least directly) with asymptotic scaling. In Table III.3 we roughly estimate the correlation length at the beginning ξ_{begin} and end ξ_{end} of the scaling windows for our three actions on an 50^2 lattice. The end of the scaling windows is due to finite size effects: lattice size and (related) spin wave problems. The practical improvement is measured by the fraction $q = \xi_{begin}/\xi_{end}$. We have $q \approx 2.5$ (1LIA), $q \approx 2.0$ (TIA) and $q \approx 1.0$ (SA). For the 1LIA asymptotic scaling sets in at the very small correlation length $\xi_{begin} \approx 2$, but we pay with early finite size effects at $\xi_{end} \approx 5$. Consequently, for the practical purposes of a mass gap calculation the TIA seems to be similarly usefull as the 1LIA, in particular because the heat-bath method is applicable for the TIA. On the other hand, both improved actions provide clearly a pratical improvement as compared with the SA. For the SA asymptotic scaling can (if at all) only be seen on lattices of size $\gtrsim 100^2$ and therefore the MC calculations are much more time consuming.

The ratio Λ_L^I/Λ_L^S has been calculated analytically /5, 8, 18, 19/ for the O(N) sigma model and the O(3) result is

$$\Lambda_L^I / \Lambda_L^S = 2.219 \ . \tag{III.6}$$

The MC simulation, however, gives

$$\Lambda_L^I / \Lambda_L^S \cong 3.0 \qquad \text{(from TIA versus SA)} \tag{III.7a}$$

and

$$\Lambda_L^I / \Lambda_L^S \cong 6.9 \qquad \text{(from 1LIA versus SA).} \tag{III.7b}$$

Particularly notable is the large difference between TIA and 1LIA. This is argued to be due to perturbative (3-loop etc.) corrections to the Λ-scale (III.4). We can easily imagine asymptotic convergence of the full lines in Fig. II.1 by a

small deviation in their slope, which cannot be numerically detected in the small scaling windows. Assuming the 1LIA estimate to be the best, a qualitative figure of the expected scaling curves was given in Ref. /19/. The 1LIA gives a result rather close to Lüschers /16/ estimate, which is based on a new finite volume method. Lüschers value is conjectured to be very close to the exact mass gap result. Strong coupling estimates /15/ are between TIA and SA (closer to TIA), and finally also variational calculations /17/ seem to approach a point, where estimates become possible.

IV. The Energy-momentum Dispersion

In our investigation we have also measured correlations between momentum $K = 0, \pm \frac{2\pi n}{L}$ $(n = 1, \ldots, \left[\frac{L}{2}\right])$ eigenstates. These correlations are defined by

$$C(K,\Delta t) = \mathrm{Re}\left\{ \langle \vec{\tilde{\phi}}(K,t)\, \vec{\tilde{\phi}}(K,t+\Delta t)\rangle \right\} \tag{IV.1}$$

where $$\vec{\tilde{\phi}}(K,t) = \sum_{x=0}^{L-1} e^{iKx}\, \vec{\phi}(x,t) ,$$

and in case of the 1LIA again the improved field (I.5) is taken. For practical reasons (disk space) we have only considered $n = \pm 1, \pm 2, \ldots, \pm 10$. Having in mind a check of the relativistic energy-momentum dispersion, i.e. the restoration of Lorentz invariance

$$E(K) = \sqrt{m^2 + K^2} , \tag{IV.2}$$

these values are the most important. From our MC data for the correlations (IV.1) we note a tendency of the Fourier transform to suppress statistical noise. This may have importance for attempts to improve mass gap estimates. In Table IV.1 we give the correlation functions for $K = \frac{14\pi}{50}$ at one value of β for each action. Notable is the strong oscillation in case of the 1LIA at short distances.

Previously the energy-momentum dispersion (IV.2) has been investigated within a variational approach (cf. Ref. /17/ and references given there). In the Figures IV.1 - IV.3 our results are summarized. We find no improvement by going from the SA to the TIA, but considereable improvement of the energy-monetum dispersion for the 1LIA. We attribute this to the diagonal terms of the 1LIA (cf. Table II.a), which are important for improving rotation invariance.

V. Correlation functions

In the previous sections we have considered the mass gap and momentum eigenstates. Other examples for quantities statisfying the RG equation (I.2) are 2- and 4-point functions

$$S_2 = \left. \frac{\delta^2 Z[J]}{\delta J_1 \, \delta J_2} \right|_{J=0} \tag{V.1}$$

$$S_4 = \left. \frac{\delta^4 Z[J]}{\delta J_1 \, \delta J_2 \, \delta J_3 \, \delta J_4} \right|_{J=0} \tag{V.2}$$

The 2-point function at zero 2-momentum is the magnetic susceptibility

$$\chi_m = S_2 (p_1 = p_2 = 0) \, . \tag{V.3}$$

It is supposed to scale like /9/

$$\chi_m = c \, (2\pi\beta)^{-4} \exp(4\pi\beta) \left(1 + O(1/\beta)\right) \, . \tag{V.4}$$

For the SA large scaling derivations in χ_m were found in Ref. /20,21/. Our present results are given in Table V.2. For the SA and the TIA they are consistent with the previous literature /8, 20, 21/. In Figure V.1 the defect $\delta_m = \beta^4 \exp(-4\pi\beta) \chi_m$ is plotted. We find a window consistent with

asymptotic scaling only for the 1LIA. This leads to the estimate

$$c \approx 0.3 \, . \tag{V.5}$$

For the SA and TIA estimates of C have to involve more hand-waving arguments. Dependence of asymptotic scaling for χ_m on the choice of the lattice action was also reported in Ref. /22/.

Finally we have also measured the "generalized susceptibility"

$$\chi_4 = \frac{S_4 (p_1 = p_2 = p_3 = p_4 = 0)}{\chi_m^2} \, , \tag{V.6}$$

which has no wave-function renormalization. On our rather large lattice the results were, however, compatible with statistical noise. For the SA and TIA data on smaller lattices were presented in /8/.

VI. Scaling behaviour of the mass gap and two-point function

As discussed in the Introduction, scaling (in general) means the validity of the RG equation (I.2) with some functions $\bar{\beta}(g)$ and $\bar{\gamma}(g)$ satisfying for $g \to 0$

$$\bar{\beta}(g) \to \bar{\beta}_{univ}(g) + O(g^4) \;, \qquad \bar{\gamma}(g) \to \bar{\gamma}_{univ}(g) + O(g^2) \;. \tag{VI.1}$$

(The regularization independent, universal parts β_{univ}, γ_{univ} are given by Eqs. (I.9-10).) In the present section we shall be concerned with "RG-invariant" functions which do not depend on wave function renormalization and hence on $\bar{\gamma}(g)$. Let us denote such a quantity, having mass dimension D, by F_D. In a lattice calculation physical quantities occur in "lattice units", that is the dimensionless function $f_D = a^D F_D$ is available (a = lattice spacing). This function can depend, in general, on different physical parameters (measured in lattice units) like e.g. $L/a = N$ (L = lattice size), $r/a = n$ (r = distance), $ap = 2\pi\nu/N$*; $\nu = 0, \pm 1, \ldots$ (p = momentum) or $aT = N_\tau^{-1}$ (T = temperature) etc.. From the RG-equation

$$\left[-a\frac{\partial}{\partial a} + \bar{\beta}(g)\frac{\partial}{\partial g}\right] F_D = 0 \tag{VI.2}$$

if follows for $f_D = f_D(g, N, n, \nu, N_\tau) = a^D F_D$

$$\left[D + N\frac{\partial}{\partial N} + n\frac{\partial}{\partial n} - \nu\frac{\partial}{\partial \nu} + N_\tau\frac{\partial}{\partial N_\tau} + \bar{\beta}(g)\frac{\partial}{\partial g}\right] f_D = 0 \;. \tag{VI.3}$$

Note, that here the variables N, n, ν, ... are considered as continuous, although on a lattice they are, of course, discrete (integer). This means that in a lattice calculation the derivatives have to be approximated by difference quotients. In the continuum limit this approximation can, however, be made arbitrarily good by using a high-order interpolation between the values obtained at neighbouring integers.

* Here we assume periodic boundary conditions.

As a simple example for the physical quantity F_D, let us consider the mass gap m_G with D = 1. The RG equation (VI.3) for $\mu_a = a m_a$ is

$$\left[1 + \bar{\beta}(g)\frac{\partial}{\partial g}\right] \mu_a(g) = 0 \;. \tag{VI.4}$$

This can be used for the calculation of the lattice β-function:

$$\bar{\beta}(g) = -\frac{\mu_a}{\frac{d\mu_a}{dg}} = -\left(\frac{d\ln\mu_a}{dg}\right)^{-1} . \tag{VI.5}$$

Note that in these equations the volume dependence of the mass gap was neglected, that is the lattice size was assumed to be very much larger than the relevant correlation length ("infinite volume limit").

Other examples for the quantities satisfying the RG equation (VI.3) can be obtained from the 2- and 4-point functions (V.1-2). The "generalized susceptibility" χ_4 defined in (V.6) has no wave function renormalization, it is dimensionless and it can depend only on the volume. On the lattice it satisfies the RG equation

$$\left[N\frac{\partial}{\partial N} + \bar{\beta}(g)\frac{\partial}{\partial g}\right] \chi_4(g, N) = 0 \;. \tag{VI.6}$$

This can, in principle, also be used to determine $\bar{\beta}(g)$, but χ_4 is rather difficult to measure numerically. Therefore, we considered the normalized two-point function as a function of the momentum

$$R_2 = \frac{S_2(ap)}{S_2(ap=0)} = \frac{S_2(ap)}{\chi_\mu} \;. \tag{VI.7}$$

(Here ap is some component of the lattice momentum having the values $ap = 2\pi\nu/N$; $\nu = 0, \pm 1, \pm 2, \ldots$.) According to Eq. (VI.3) and neglecting the volume

dependence, R_2 satisfies

$$\left[-\nu\frac{\partial}{\partial\nu}+\bar\beta(g)\frac{\partial}{\partial g}\right]R_2(g,\nu)=0\,. \tag{VI.8}$$

This implies

$$\bar\beta(g)=\frac{\frac{\partial}{\partial\ln\nu}R_2}{\frac{\partial}{\partial g}R_2}\,. \tag{VI.9}$$

Measuring the two-point function R_2 at different values of g and ν allows, therefore, a numerical determinattion of the lattice $\bar\beta$-function.

The equations like (VI.6) or (VI.8) imply that the functions χ_4 and R_2 depend only on a particular combination of the two arguments. For instance, the solution of Eq. (VI.8) is, with an arbitrary function $r_2(x)$,

$$R_2=r_2\left(\ln\nu+\int^g\frac{dg'}{\bar\beta(g')}\right)\,. \tag{VI.10}$$

This property can be easily checked graphically. A convenient choice is to plot $\ln R_2$ as a function of ln(ap) and to try to bring the curves belonging to the different coupling constant values on top of each other by a shift in ln(ap). If this can be achieved there is scaling, the obtained universal curve is the continuum $\ln R_2$ function and the lattice $\bar\beta$-function can also be extracted from the shifts. The result of this procedure for the case of the SA and 1LIA is shown on Figs. VI.1-2. As it can be seen, the result is a rather nice scaling curve, in spite of the large violations of asymptotic scaling observed for the SA in the previous sections. There are, of course, also small scaling violations

seen in Fig. VI.1 but the corresponding curve for the 1LIA (and also for TIA) is so similar, that one cannot draw an immediate conclusion concerning the quality of scaling in the three cases. The crucial question is, whether the lattice $\bar\beta$-function obtained from the normalized 2-point function R_2 is universal (as it should be), that is whether it describes the scaling behaviour of all the quantitites on the theory.

In order to study these questions quantitatively, we numerically determined the lattice $\bar\beta$-function for all the three actions using the equations (VI.5) and (VI.9). The derivatives were estimated from a quadratic extrapolation using the two neighbouring values in g and $\ln\nu$. The obtained results are collected in Table VI.1. As it can be seen, the lattice $\bar\beta$-function for SA is rather different from the asymptotically valid universal part (I.9) even at the smallest measured values of the coupling g. This explains the observed large deviations from asymptotic scaling. The 1LIA comes at $g^{-1}\simeq\beta=0.9$ rather near to $\bar\beta_{univ}$ (it actually coincides with $\bar\beta_{univ}$ within errors). The TIA is between SA and 1LIA. The universality of the $\bar\beta$-function values, obtained from the mass gap and from different momenta, is very good at $\beta=0.9$ for the 1LIA and at $\beta=1.2$ for the TIA. In the other points the numbers are in most cases compatible with universality within errors. An exception is $\beta=0.9$ for the SA and perhaps $\beta=0.7$ for the 1LIA.

In summary: the behaviour of the measured quantities is much better compatible with scaling if the lattice $\bar\beta$-function is not fixed to the universal (asymptotic) part $\bar\beta_{univ}$. The $\bar\beta$-function at the smallest measured values of the coupling are nearly equal to $\bar\beta_{univ}$ for TIA and 1LIA but otherwise $\bar\beta(g)$ is different from $\bar\beta_{univ}$. Scaling (in general) holds better for the improved actions than for the standard one, but with the present errors it is not possible to distinguish numerically between the quality of scaling for the different actions.

VII. Summary and conclusions

We have carried out MC calculations for the 2d O(3) non-linear σ-model with three different actions: standard action (SA), Symanzik's tree-level improved action (TIA) and 1-loop improved action (1LIA). The 1LIA behaves much better with respect to asymptotic scaling. Most likely this is an accident, because Symanzik's improvement is made for mass ratios (scaling in general sense) but not for asymptotic scaling.

Scaling in the general sense is also investigated. The numerically determined values of the lattice $\bar{\beta}$-function $\bar{\beta}(g)$ agree reasonably well if calculated from different physical quantities (although $\bar{\beta}(g)$ is quite different for the three actions). It is expected that the agreement is better for the improved actions, but within the statistical noise of our MC investigation this is practically invisible.

Another aspect of (general) scaling, namely the restoration of Lorentz-invariance in the energy-momentum dispersion, is found to be considerably better for the 1LIA than for the other two actions. This is presumably due to the off-diagonal terms present in the 1LIA. Lorentz-invariance (in particular also rotation invariance, which we did not investigate in this paper) is a very essential requirement.

In summary: the improved actions have lead to a better understanding of MC problems in reaching the continuum limit and established a number of interesting features. MC results /23-25/ for the 4d SU(2) TIA indicate possible improvements which are in the spirit of Symanzik's program (asymptotic scaling is not improved, however).

Acknowledgement: We thank Prof. K. Symanzik for his constant interest and advise.

References

/1/ S.K. Ma, Phys. Rev. Lett. 37 (1976) 461;
R. Swendson, Phys. Rev. Lett. 42 (1979) 859.

/2/ K.G. Wilson, Cargèse lectures 1979, edited by G. 't Hooft et al., Plenum Press, New York, 1980.

/3/ S.H. Shenker, J. Tobochnik, Phys. Rev. B22 (1980) 4462.

/4/ K. Symanzik, in: "Mathematical Problems in Theoretical Physics", Eds. R. Schrader et al. (Lecture Notes in Physics 153, Springer, Berlin, 1982);
K. Symanzik, "Continuum limit and improved action in lattice theories I: Principles and ϕ^4 theory", Preprint, DESY 83-016.

/5/ K. Symanzik, "Continuum limit and improved action in lattice theories II: O(N) non-linear sigma model in perturbation theory", Preprint, DESY 83-026.

/6/ G. Martinelli, G. Parisi, R. Petronzio, Phys. Lett. 114B (1982) 251.

/7/ B. Berg, S. Meyer, I. Montvay, K. Symanzik, Phys. Lett. 126B (1983) 467.

/8/ M. Falcioni, G. Martinelli, M.L Paciello, B. Taglienti, G. Parisi, Preprint (1983).

/9/ E Brézin, J. Zinn-Justin, Phys. Rev. B14 (1976) 3110.

/10/ B. Berg and A. Billoire, Nucl. Phys. B221 (1983) 109 and Nucl. Phys. B (to be published).

/11/ K. Binder, in Phase Transitions and Critical Phenomena, eds. C. Domb and M.S. Green, Vol. 5 (Academic Press, New York, 1976).

/12/ G. Fox, R. Gupta, O. Martin, S. Otto, Nucl. Phys. B205 [FS5] (1982) 188.

/13/ M. Fukugita, Y. Oyanagi, Phys. Lett. 123B (1983) 71.

/14/ R. Gupta, Preprint, CALT-68-1010 (1983).

/15/ J. Shigemitsu and J.B. Kogut, Nucl. Phys. B190 [FS3] (1981) 365;
R. Musto, F. Nicodemi and R. Pettorino, Nucl. Phys. B210 [FS6] (1982) 263.
For previous work see: D.N. Lambeth and H.E. Stanley, Phys. Rev. B12 (1975) 5302.

/16/ M. Lüscher, Phys. Lett. 118B (1982) 391.

/17/ A. Patkós, Preprint, Eötvös University, July 1983.

/18/ Y. Iwasaki and T. Yoshie, University of Tsukuba, Ibaraki preprint, UTHEP-94 (1982), (unpublished).

/19/ B. Berg, Preprint, DESY 83-031, to be published in Z. Phys. C.

/20/ G. Martinelli, G. Parisi, R. Petronzio, Phys. Lett. 100B (1981) 485.

/21/ B. Berg and M. Lüscher, Nucl. Phys. B180 [FS3] (1981) 412.

/22/ Y. Iwasaki and T. Yoshie, Phys. Lett. 125B (1983) 201.

/23/ S. Belforte, G. Curci, P. Menotti and G.P. Paffuti, Preprint IFUH-TH 83/6, Pisa.

M. Fukugita, T. Kaneko, T. Niuya and A. Ukawa, Preprint INS-REP. 473 (1983) and Addendum.

/24/ B. Berg, A. Billoire, S. Meyer and C. Panagiotakopoulos, Preprint, DESY 83-057 (Phys. Lett. B., to appear), and in preparation.

/25/ F. Gutbrod and I. Montvay, in preparation.

Figure captions

Fig. III.1: The mass gap.

Fig. III.2: The mass gap defect.

Fig. IV.1: Energy-momentum dispersion for the SA.

Fig. IV.2: Energy-momentum dispersion for the TIA.

Fig. IV.3: Energy-momentum dispersion for the 1LIA.

Fig. V.1: Scaling defect for the magnetic susceptibility.

Fig. VI.1: Test of scaling for the SA.

Fig. VI.2: Test of scaling for the 1LIA.

Table 1

The coefficients C_i^1

i	C_i^1
1	- 0.0048591
2	- 0.0285844
3	0.
4	- 0.0023988
5	- 0.0245659
6	- 0.0032718
7	0.
8	- 0.0087486
9	+ 0.0194364

Table 2a

Coefficients of bilinear interactions

b_i	S_i^b	i
$0.4892\ g + {}^4/3$	$\phi_j\ \phi_{j+\hat{\mu}}$	1
$-\ 0.0945\ g - {}^1/12$	$\phi_j\ \phi_{j+2\hat{\mu}}$	2
$-\ 0.0983\ g$	$\phi_j\ \phi_{j+\hat{\mu}+\hat{\nu}}\quad (\mu \neq \nu)$	3

Table 2b

Coefficients of quadrilinear interactions

q_i	S_i^q	i
$-\ 0.0175\ g$	$(\phi_j\ \phi_{j+\hat{\mu}})^2\ ,\quad (\phi_j\ \phi_{j+\hat{\mu}})(\phi_j\ \phi_{j-\hat{\mu}})\ ,$	1,2
	$(\phi_j\ \phi_{j+\hat{\mu}})(\phi_{j+\hat{\mu}}\ \phi_{j+2\hat{\mu}})$	3
$+\ 0.0194\ g$	$(\phi_j\ \phi_{j+2\hat{\mu}})^2\ ,\quad (\phi_j\ \phi_{j+\hat{\mu}+\hat{\nu}})^2\ ,$	4,5
	$-(\phi_j\ \phi_{j+\hat{\mu}+\hat{\nu}})(\phi_j\ \phi_{j-\hat{\mu}-\hat{\nu}})\ ,\ -(\phi_j\ \phi_{j+\hat{\mu}+\hat{\nu}})(\phi_{j+\hat{\mu}+\hat{\nu}}\ \phi_{j+2\hat{\mu}})$	6,7
	$-(\phi_j\ \phi_{j+\hat{\mu}+\hat{\nu}})(\phi_{j+\hat{\mu}+\hat{\nu}}\ \phi_{j+2\hat{\mu}})\ ,$	8
	$(\phi_j\ \phi_{j+\hat{\mu}+\hat{\nu}})(\phi_{j+\hat{\mu}-\hat{\nu}}\ \phi_{j+2\hat{\mu}})\ ,$	9
	$(\phi_j\ \phi_{j+\hat{\mu}+\hat{\nu}})(\phi_{j-\hat{\mu}+\hat{\nu}}\ \phi_{j+2\hat{\mu}})\ ,\qquad (\mu \neq \nu)\ .$	10

Table 3a

E and statistics for the SA

β	E	Sweeps
0.4	.1366 ± .0002	9 000
0.8	.2920 ± .0001	18 200
0.9	.3351 ± .0001	18 200
1.0	.3801 ± .0002	18 200
1.1	.4264 ± .0002	18 200
1.2	.4728 ± .0003	18 200
1.3	.5188 ± .0003	18 200
1.4	.5621 ± .0003	15 400
1.5	.6016 ± .0002	18 000
1.6	.6364 ± .0003	18 200
1.8	.6886 ± .0002	16 100

100^2 lattice:

1.4	.5620 ± .0001	20 800
1.5	.6016 ± .0002	21 200

Table 3b

E and statistics for the TIA

β	E	Sweeps
0.8	.3820 ± .0002	15 400
0.9	.4349 ± .0002	14 600
1.0	.4879 ± .0002	18 000
1.1	.5382 ± .0002	18 000
1.2	.5852 ± .0003	18 000
1.25	.6068 ± .0004	18 000
METROPOLIS		
0.8	.3817 ± .0002	18 000

Table 3c

E and statistics for the 4LIA

β	E	Sweeps
0.6	.3950 ± .0003	22 200
0.7	.4424 ± .0004	18 000
0.8	.4812 ± .0002	21 900
0.9	.5362 ± .0009	21 000
1.0	.5834 ± .0007	18 000
1.1	.6297 ± .0011	31 800

Table II.1

Correlation functions at selected values of β

Δt	β=1.2 , SA	β=1.6 , SA	β=1.1 , TIA	β=0.8 , 1LIA
0	3.431 ± 0.023	11.4 ± 0.2	4.125 ± 0.027	3.056 ± 0.016
1	2.504 ± 0.023	10.7 ± 0.2	3.278 ± 0.027	1.779 ± 0.015
2	1.833 ± 0.023	10.2 ± 0.2	2.534 ± 0.025	1.136 ± 0.015
3	1.341 ± 0.022	9.6 ± 0.2	1.948 ± 0.024	0.657 ± 0.015
4	0.981 ± 0.020	9.1 ± 0.2	1.489 ± 0.021	0.381 ± 0.016
5	0.719 ± 0.018	8.7 ± 0.3	1.131 ± 0.019	0.229 ± 0.016
6	0.529 ± 0.016	8.3 ± 0.3	0.852 ± 0.019	0.132 ± 0.014
7	0.389 ± 0.014	7.9 ± 0.3	0.634 ± 0.018	0.081 ± 0.011
8	0.286 ± 0.012	7.6 ± 0.3	0.464 ± 0.018	0.050 ± 0.009
9	0.214 ± 0.010	7.3 ± 0.3	0.334 ± 0.018	0.030 ± 0.007
10	0.162 ± 0.010	7.0 ± 0.3	0.239 ± 0.021	0.021 ± 0.007
11	0.123 ± 0.011	6.8 ± 0.3	0.169 ± 0.023	0.011 ± 0.007
12	0.095 ± 0.011	6.5 ± 0.3	0.117 ± 0.026	0.010 ± 0.008
13	0.074 ± 0.011	6.3 ± 0.3	0.081 ± 0.028	0.005 ± 0.009
14	0.059 ± 0.010	6.1 ± 0.3	0.057 ± 0.029	0.003 ± 0.009
15	0.044 ± 0.010	6.0 ± 0.3	0.043 ± 0.030	0.000 ± 0.012
16	0.030 ± 0.011	5.8 ± 0.3	0.032 ± 0.032	0.004 ± 0.011
17	0.017 ± 0.012	5.7 ± 0.3	0.026 ± 0.035	0.006 ± 0.011
18	0.008 ± 0.014	5.5 ± 0.3	0.022 ± 0.038	0.003 ± 0.010
19	0.001 ± 0.016	5.4 ± 0.4	0.021 ± 0.041	0.001 ± 0.011
20	- 0.007 ± 0.018	5.3 ± 0.4	0.023 ± 0.043	0.003 ± 0.011
21	- 0.013 ± 0.020	5.3 ± 0.4	0.029 ± 0.046	- 0.002 ± 0.012
22	- 0.016 ± 0.021	5.2 ± 0.4	0.036 ± 0.049	- 0.005 ± 0.013
23	- 0.015 ± 0.023	5.2 ± 0.4	0.041 ± 0.051	- 0.007 ± 0.013
24	- 0.013 ± 0.024	5.2 ± 0.4	0.044 ± 0.052	- 0.007 ± 0.014
25	- 0.014 ± 0.024	5.1 ± 0.4	0.046 ± 0.052	- 0.009 ± 0.015

Table II.2

Mass gap estimates (mean values) from the correlations of Table II.1.

Δt	β=1.2 , SA	β=1.6 , SA	β=1.1 , TIA	β=0.8 , 1LIA
1	0.315	0.063	0.23	0.54
2	0.313	0.056	0.24	0.50
3	0.313	0.057	0.25	0.51
4	0.313	0.056	0.25	0.52
5	0.313	0.054	0.26	0.52
6	0.312	0.053	0.26	0.52
7	0.311	0.052	0.27	0.52
8	0.311	0.051	0.27	0.51
9	0.308	0.050	0.28	0.51
10	0.305	0.049	0.28	0.50
11	0.302	0.047	0.29	0.51
12	0.298	0.047	0.30	0.48
13	0.294	0.046	0.30	
14	0.290	0.045	0.30	
15	0.291	0.043	0.30	
16	0.296	0.042		
17	0.312	0.041		
18		0.040		
19		0.039		
20		0.038		
21		0.036		
22		0.036		
23		0.034		
24		0.033		
25		0.032		

Table II.3

Asymptotic Scaling windows on an 50^2 lattice

	ξ_{begin}	ξ_{end}
SA	7	7
TIA	4	8
1LIA	2	5

Table IV

Correlations for $K = \frac{14\pi}{50}$ eigenstates

Δt	SA , β=1.0	TIA , β=0.8	1LIA , β=0.6
0	1.220 ± 0.002	1.279 ± 0.002	2.82 ± 0.02
1	0.458 ± 0.002	0.502 ± 0.002	- 0.56 ± 0.01
2	0.172 ± 0.001	0.171 ± 0.002	0.17 ± 0.01
3	0.065 ± 0.001	0.056 ± 0.001	0.08 ± 0.01
4	0.026 ± 0.001	0.018 ± 0.001	0.01 ± 0.01
5	0.011 ± 0.001	0.006 ± 0.001	- 0.01 ± 0.01
6	0.004 ± 0.001	0.002 ± 0.001	

Table V

Magnetic susceptibilities

SA:

β	χ_m
0.4	1.80 ± 0.03
0.8	4.59 ± 0.08
0.9	6.35 ± 0.14
1.0	9.28 ± 0.30
1.1	13.4 ± 0.4
1.2	22.1 ± 0.6
1.3	42.8 ± 3.0
1.4	84.0 ± 5.0
1.5	181.0 ± 14.0
1.6	350.0 ± 13.0
1.8	687.0 ± 10.0

100^2 lattice

1.4	70.1 ± 4.7
1.5	171.0 ± 20.0

TIA:

β	χ_m
0.8	7.7 ± 0.2
0.9	10.9 ± 0.4
1.0	31.7 ± 1.2
1.2	64.6 ± 5.1
1.25	97.0 ± 12.0

METROPOLIS:

0.8	7.4 ± 0.2

1LIA:

β	χ_m
0.6	5.42 ± 0.14
0.7	8.19 ± 0.26
0.8	12.1 ± 0.4
0.9	22.9 ± 2.2
1.0	50.0 ± 8.0
1.1	193.0 ± 43.0

Table VI

Numerical values of the $\bar{\beta}(g)$ function (always $-\bar{\beta}$ is given) obtained from Eqs. (VI.5), (VI.9).

	$\beta=g^{-1}$	μ_G	$\nu=4$	$\nu=6$	$\nu=8$	$\nu=10$	$\nu=12$	$\nu=14$	$\nu=16$	$\nu=18$	$-\beta_{univ}$
SA	0.9	0.51±.03	0.32 ±.04	0.38 ±.04	0.45 ±.03	0.48 ±.02	0.45 ±.02	0.44 ±.02	0.46 ±.02	0.40 ±.02	0.231
	1.0	0.38±.03	0.43 ±.04	0.37 ±.03	0.36 ±.02	0.38 ±.01	0.39 ±.01	0.36 ±.01	0.35 ±.01	0.37 ±.02	0.184
	1.1	0.29±.03	0.28 ±.03	0.27 ±.02	0.28 ±.02	0.27 ±.01	0.26 ±.01	0.28 ±.01	0.26 ±.01	0.25 ±.01	0.151
	1.2	0.19±.02	0.164±.014	0.162±.007	0.184±.007	0.181±.006	0.174±.006	0.174±.004	0.181±.006	0.168±.006	0.125
	1.3	0.15±.02	0.145±.009	0.137±.005	0.138±.005	0.145±.006	0.137±.006	0.132±.005	0.138±.006	0.136±.005	0.106
1LIA	0.7	0.62±.07	0.37 ±.09	0.58 ±.09	0.62 ±.07	0.62 ±.07	0.55 ±.05	0.58 ±.03	0.57 ±.03	0.49 ±.04	0.399
	0.8	0.45±.06	0.30 ±.05	0.30 ±.04	0.35 ±.03	0.37 ±.03	0.40 ±.03	0.38 ±.02	0.38 ±.02	0.38 ±.02	0.298
	0.9	0.23±.05	0.20 ±.03	0.23 ±.02	0.24 ±.01	0.24 ±.01	0.26 ±.02	0.25 ±.02	0.25 ±.02	0.24 ±.02	0.231
TIA	0.9	0.32±.03	0.35 ±.05	0.37 ±.03	0.39 ±.04	0.39 ±.03	0.38 ±.02	0.37 ±.03	0.37 ±.02	0.39 ±.02	0.231
	1.0	0.29±.03	0.36 ±.04	0.29 ±.04	0.29 ±.03	0.27 ±.03	0.30 ±.04	0.29 ±.03	0.27 ±.02	0.28 ±.02	0.184
	1.1	0.21±.04	0.19 ±.03	0.21 ±.03	0.22 ±.02	0.21 ±.02	0.20 ±.03	0.21 ±.02	0.19 ±.02	0.20 ±.01	0.151
	1.2	0.16±.06	0.15 ±.03	0.14 ±.02	0.14 ±.02	0.15 ±.02	0.15 ±.02	0.15 ±.01	0.14 ±.01	0.15 ±.01	0.125

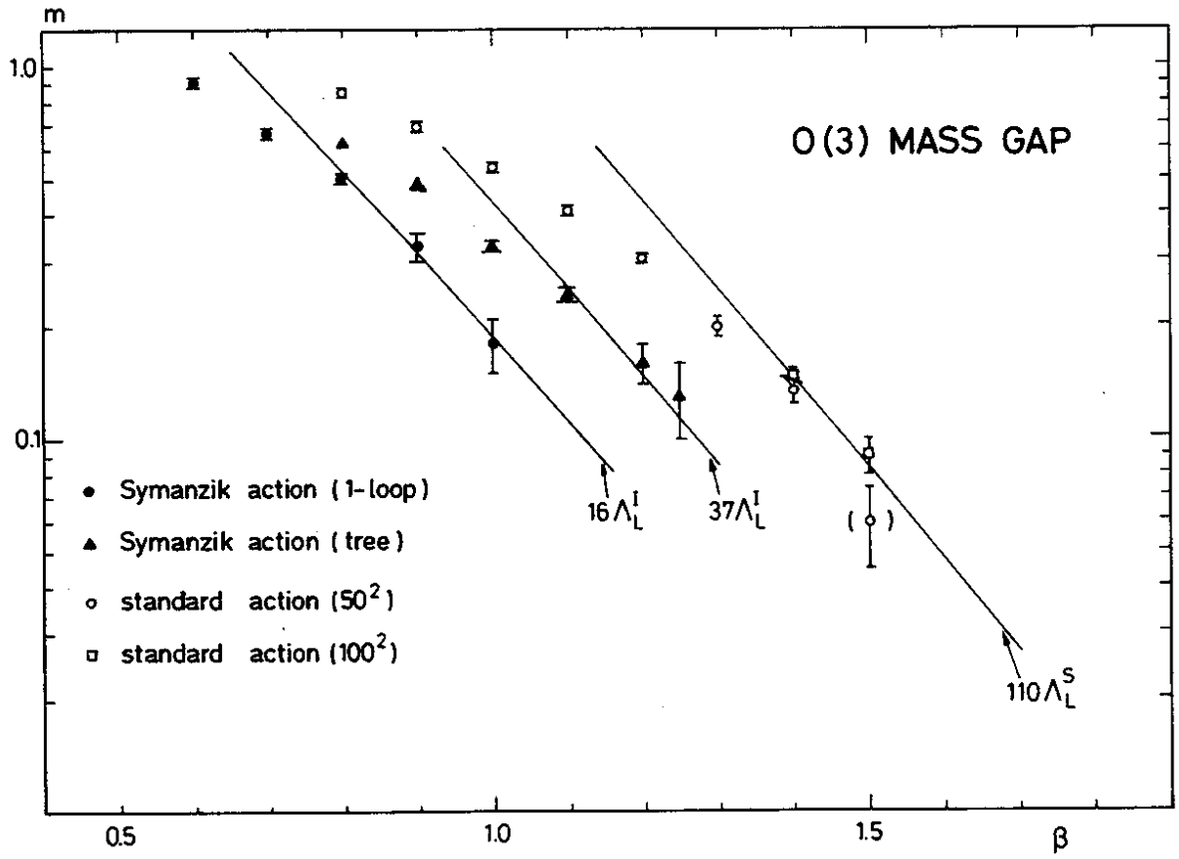

Fig. III.1.

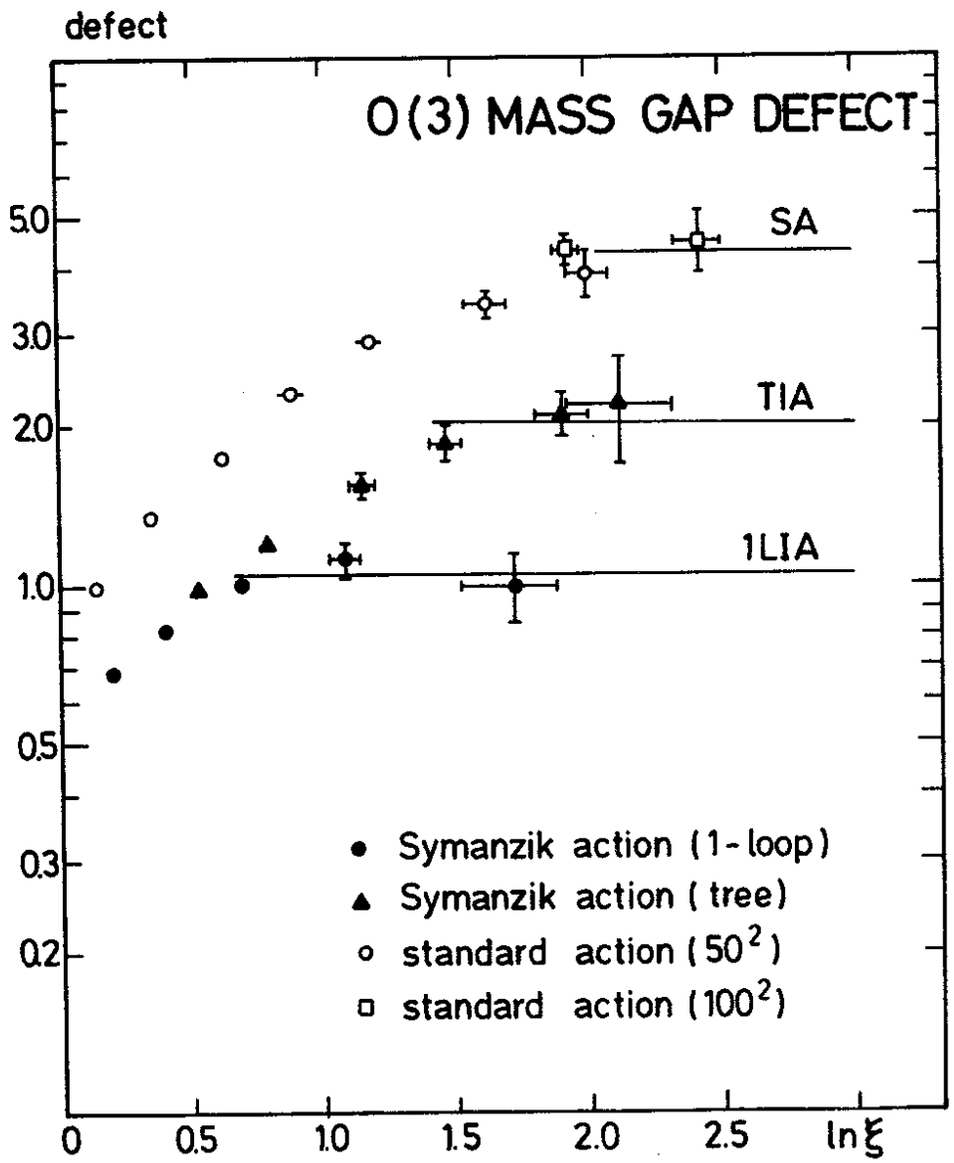

Fig. III. 2.

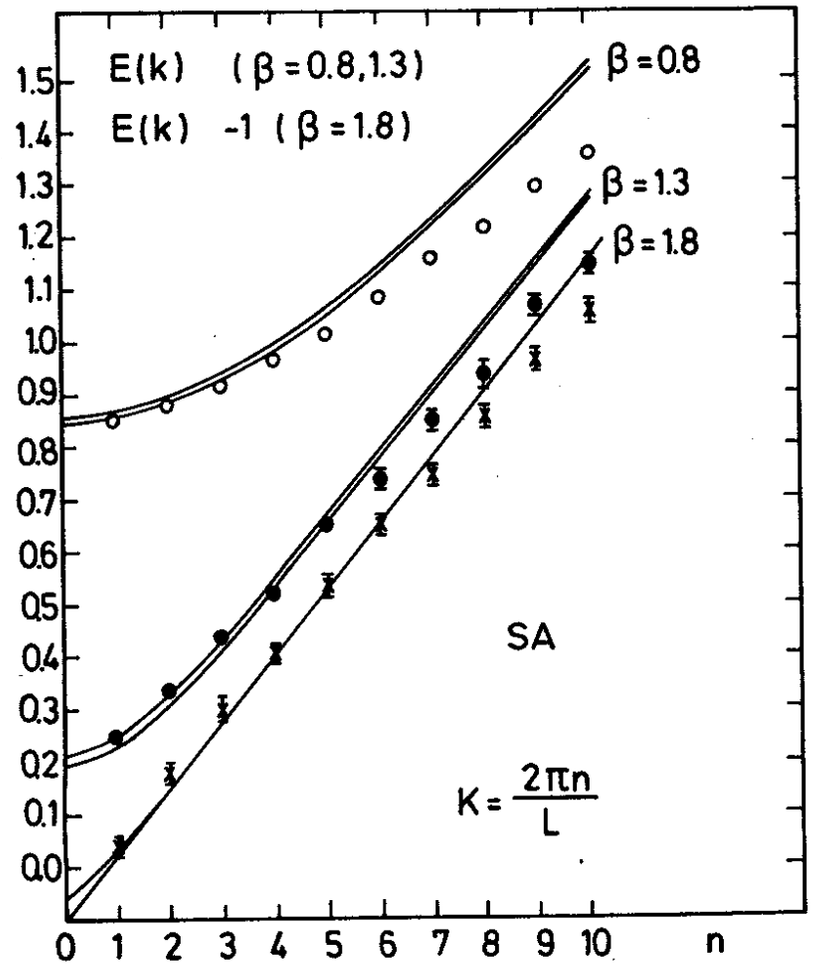

Fig. IV. 1

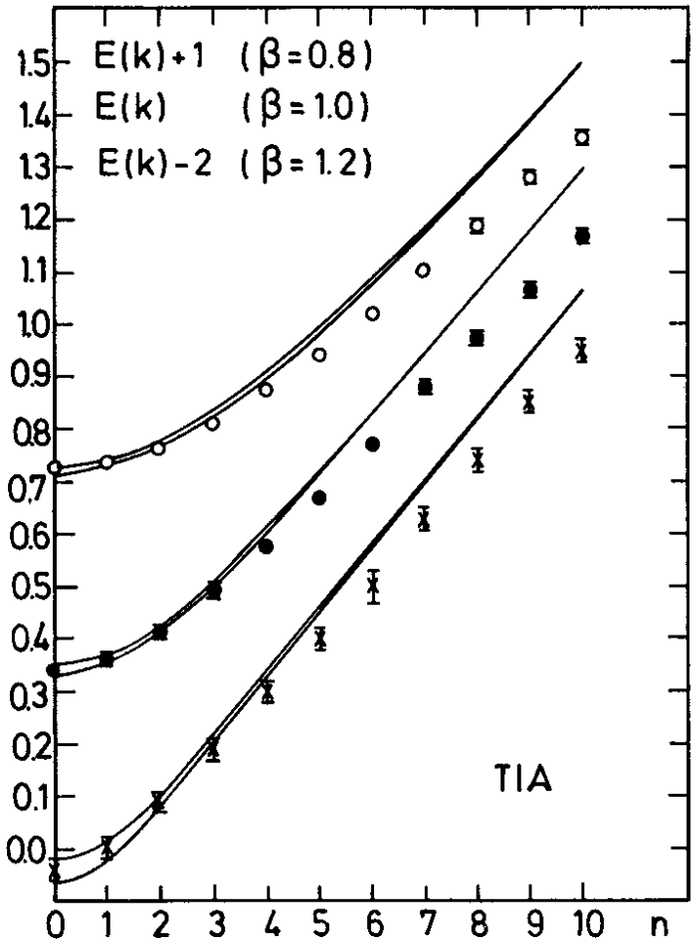

Fig. IV. 2

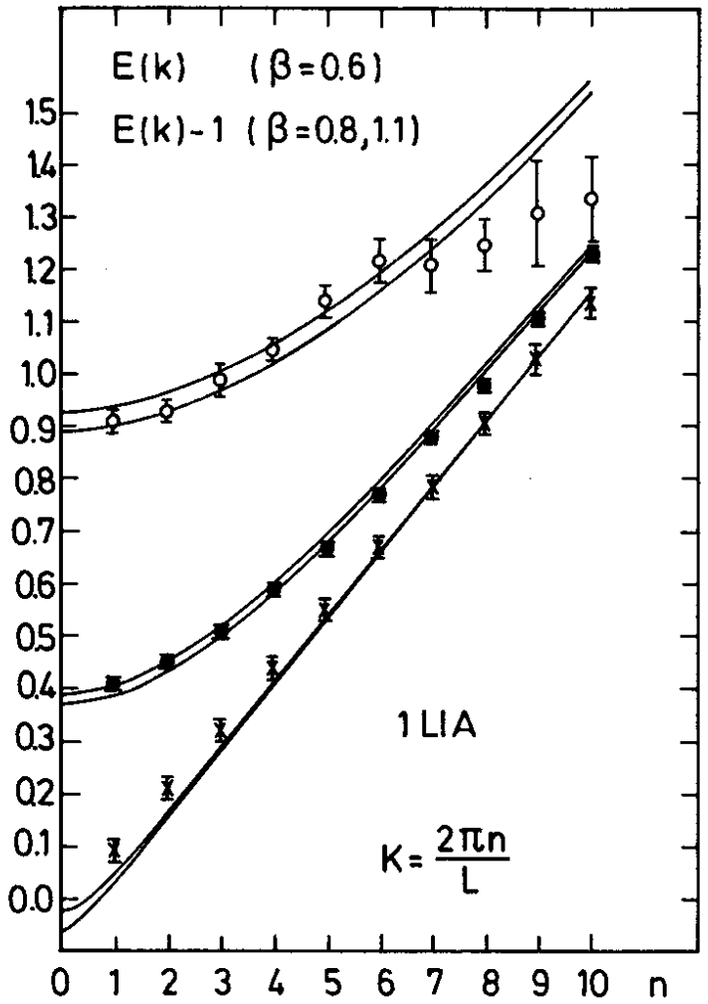

Fig. IV. 3

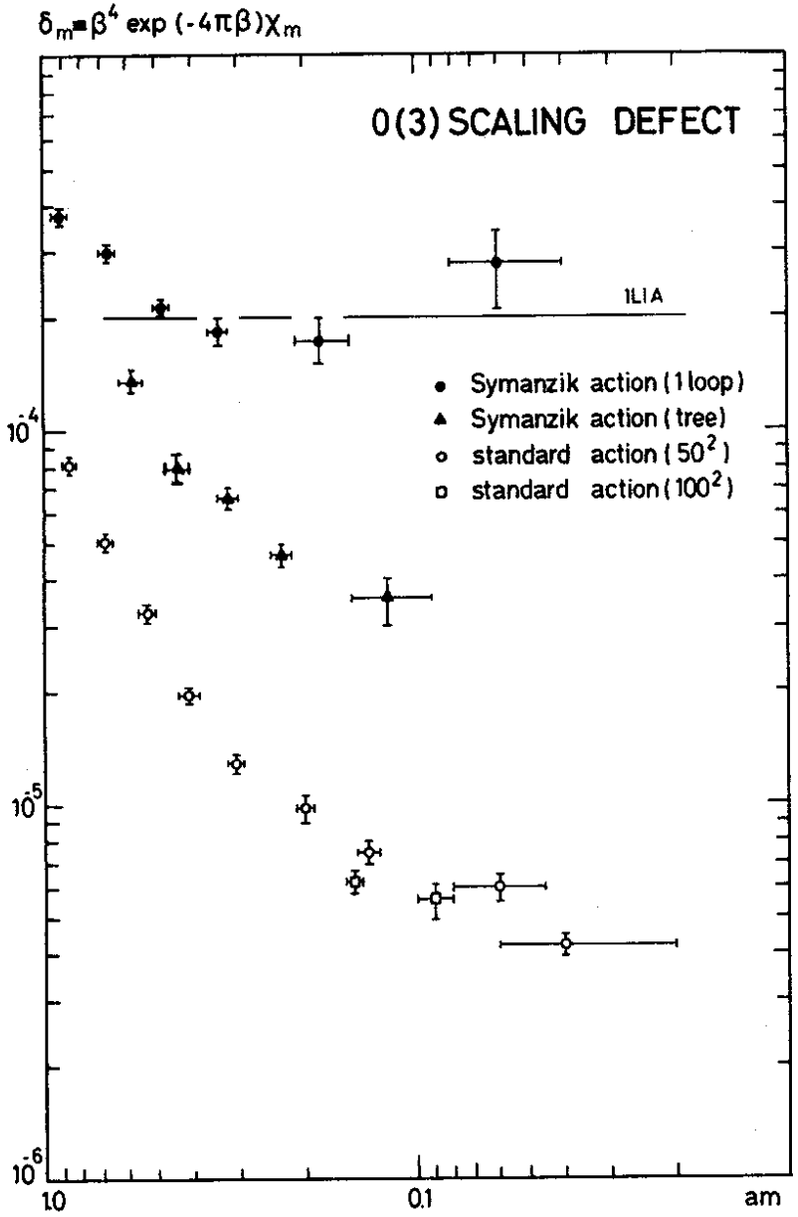

Fig. V. 1.

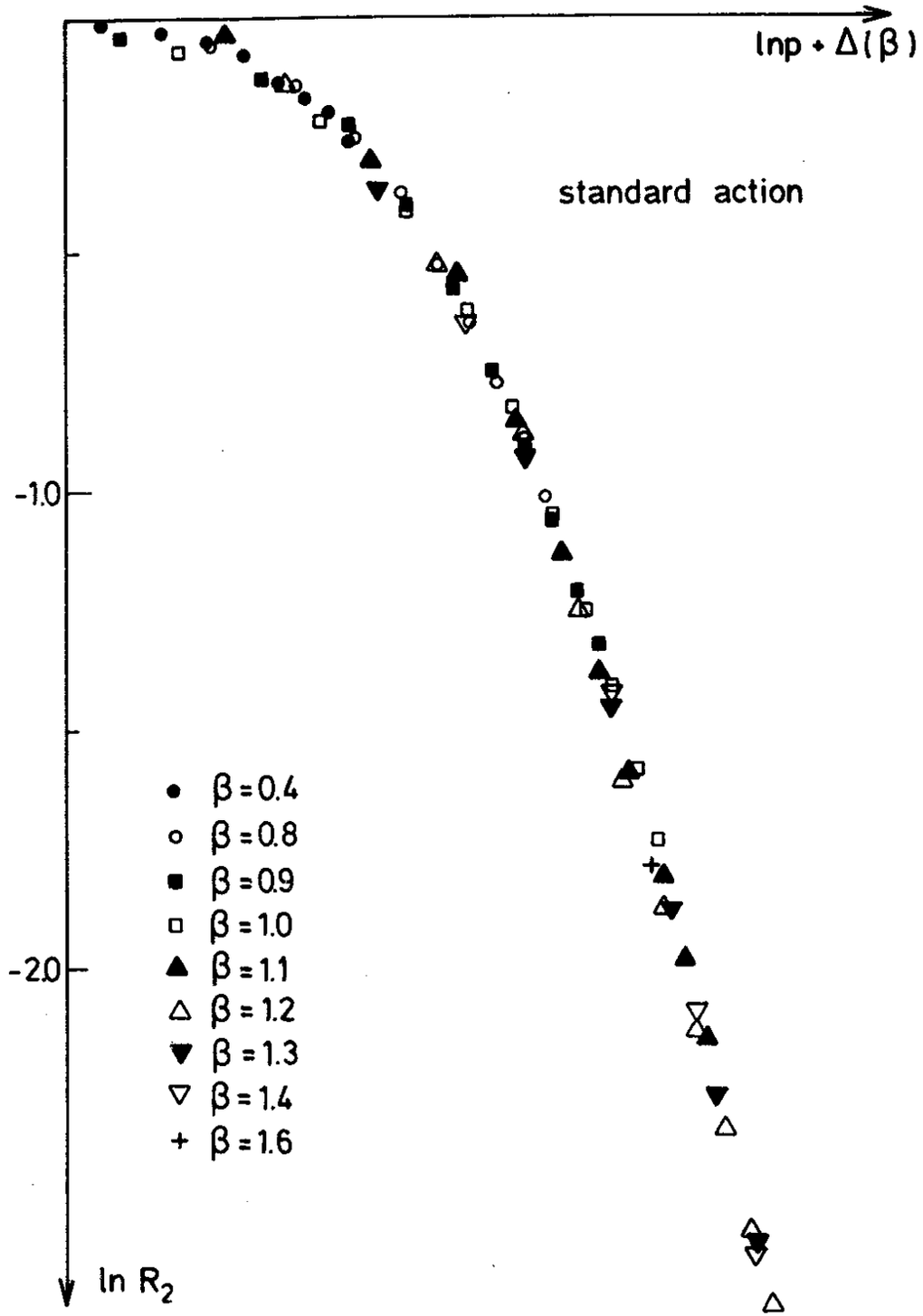

Fig. VI. 1

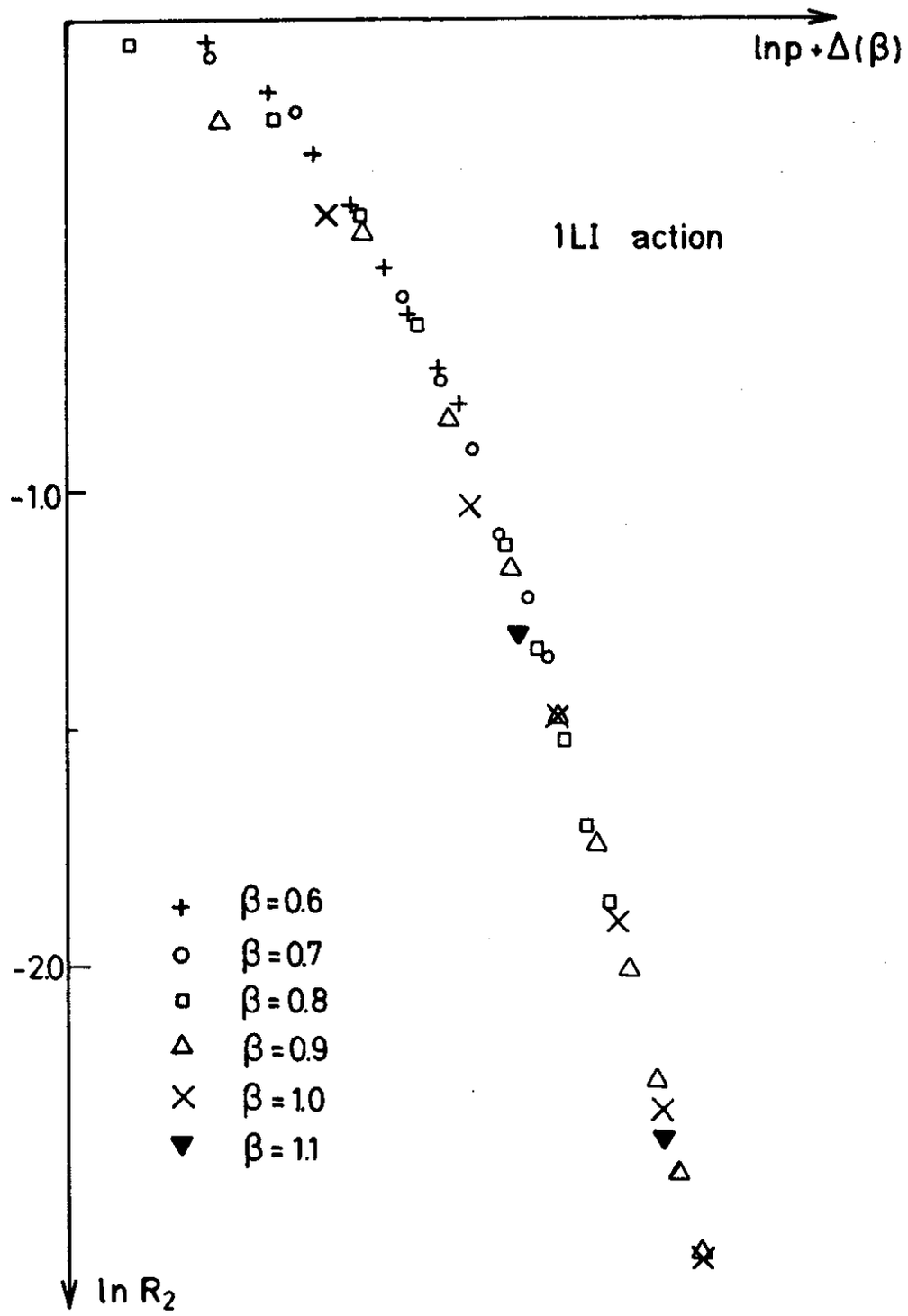

Fig. VI. 2.